UCRL-TR-202501

LAWRENCE LIVERMORE NATIONAL LABORATORY

Enhancement of Strength and Ductility in Bulk Nanocrystalline Metals

T.G. Nieh, Cristopher A. Schuh, Maria Jose Caturla, Andrea m Hodge

February 24, 2004

Disclaimer

This work was performed under the auspices of the U.S. Department of Energy by University of California, Lawrence Livermore National Laboratory under Contract W-7405-Eng-48.

Materials Synthesis Characterization and Processing

Enhancement of Strength and Ductility in Bulk Nanocrystalline Metals

Tai-Gang Nieh
Christopher A. Schuh
Maria Jose Caturla
Andrea M. Hodge
LLNL Directorate: Chemistry and Materials Science
01-ERD-085

Purpose

The purpose of this project is to develop a robust scientific and technological framework for the design of high-strength and -ductility nanocrystalline materials for applications of technical importance to the Laboratory. The project couples theory and experiments with an emphasis on materials of macroscopic dimensions (mm to cm) that are composed of nanoscale (<100 nm) grains. There are four major tasks: (1) synthesize nanocrystalline materials with grain size in the 5- to 100-nm range; (2) conduct experimental studies to probe mechanisms of mechanical deformation and failure; (3) use large-scale simulation modeling technologies to provide insight to deformation mechanisms that may not be observable experimentally; and (4) check the results obtained from modeling, comparing experimental observations with results obtained from atomistic and dislocation-based simulations.

This project supports efforts within the Stockpile Stewardship Program (SSP) to understand and predict properties of metals such as strength and ductility.

Activities

Experiments

We synthesized nanocrystalline nickel using electrodeposition method, as shown in a typical high-resolution transmission electron image in Fig. 1. The abrasion resistance of electrodeposited nanocrystalline nickel was subsequently investigated using the nano-scratch technique with a ramping load. At the finest grain sizes studied (12-14 nm), a breakdown in Hall-Petch hardening is observed directly in hardness data, as shown in Fig. 2. The data indicate the breakdown occurs at a grain size of about 14 nm. The changes in abrasive wear behavior are quantitatively commensurate with the changes in hardness, despite the apparent transition in deformation mechanisms at the finest grain sizes. We therefore demonstrated unequivocally the breakdown of the classical Hall-Petch relationship in nickel with grain sizes in the nm scale.

It is recognized that pure metals with grain sizes below about 10 nm are very difficult to prepare, however, alloying enables the realization of finer grain sizes, often down to the amorphous limit. In our project, the role of solid solution additions of ~13 at% W to nanocrystalline Ni was considered for electrodeposited alloys with grain sizes below 10 nm. We analyzed the structure of the nanocrystalline alloys using high-resolution transmission electron microscopy, and related to the mechanical properties assessed by instrumented nanoindentation and nano-scratch experiments. The Ni-W alloys exhibit higher hardness and scratch resistance as compared to the finest pure nanocrystalline Ni alloys, although the contribution of solid solution strengthening from W is expected to be essentially negligible; this is shown in Fig. 3. The improved properties are therefore attributable to the finer length scale available in multicomponent nanocrystalline alloys, and suggest that alloying may suppress the breakdown of Hall-Petch strengthening to finer grain sizes. Finally, our data are shown to smoothly bridge the hardness-grain size trend between nanocrystalline Ni (grain size > 10 nm) and amorphous Ni-based alloys.

Simulations

We studied two aspects: effect of variation of type of grain boundary on deformation and strength asymmetry. In the case of type of grain boundary, we performed molecular dynamics simulations and found significant differences in the deformation mechanisms of nanocrystalline nickel with low and high angle boundaries. For the case studied with average grain size of 12 nm, low angle boundaries present enhanced dislocation activity and reduced strength with respect to high angle boundaries for low strains. In the latter most of the deformation is accommodated at the grain boundaries with limited dislocation activity, while in the case of low angle boundaries most of the displacements observed are associated with the motion of partial dislocations nucleated at the grain boundaries. These results are summarized in Fig. 4.

In the case of strength asymmetry, we use static molecular simulations to explore asymmetries in the plastic flow of idealized nanocrystalline nickel. We found that both the yield and flow stresses of these materials are higher in compression than in tension, as shown in Fig. 5. This result indicates that the finest nanocrystalline metals require some pressure or normal stress dependent term in their global yield criterion. Specifically, one could consider the classical Mohr-Coulomb criterion for the finest nanocrystalline metals, instead of the conventional von Mises criterion. Our results also support an analogy between the deformation mechanisms in the finest nanocrystalline metals and those in amorphous metals, which give rise to tension/compression asymmetry.

Technical outcomes

This project results in the installation of an advanced electrodeposition facility in house. Use this facility, we successfully developed the capability of producing nanocrystalline metals, such as nickel, nickel-tungsten alloy and copper. This unit is readily to modify to produce structures of importance to the lab. We not only gained experiences in producing nanocrystalline metals but also developed a better understanding of the physical/mechanical behavior of nanocrystalline metals. The knowledge can be transferable to DOE projects.

The following publications were published or submitted during the course of this project:

C. Schuh, T. G. Nieh, and T. Yamasaki, 'Hall-Petch Breakdown Manifested in Abrasive Wear Resistance of Nanocrystalline Nickel,' *Scripta Mater*. 46, 735-740 (2002).

C. A. Schuh and T. G. Nieh, 'A Nanoindentation Study of Serrated Flow in Bulk Metallic Glasses,' *Acta Mater*. 51(1), 87-99 (2003).

C.A. Schuh, T.G. Nieh, and H. Iwasaki, 'The Effect of Solid Solution W Additions on the Mechanical Properties of Nanocrystalline Ni,' *Acta Mater*. 51(2), 432-443 (2003).

C.A. Schuh, A.S. Argon, T.G. Nieh, and J. Wadsworth, 'The Transition from Localized to Homogeneous Plasticity during Nanoindentation of an Amorphous Metal,' *Phil. Mag. A*. 83(22), 2585-2597 (2003).

H Iwasaki, K Higashi, and T.G. Nieh, 'Tensile deformation and microstructure of a nanocrystalline Ni-W alloy produced by electrodeposition,' *Scripta Mater*, 50(3), 395-399 (2003).

A.C. Lund, T.G. Nieh, and C.A. Schuh, 'Tension/Compression Strength Asymmetry in a Simulated Nanocrystalline Metal,' *Phys. Rev. B* 69, 012121-1-4 (2004).

M.-J. Caturla, T.G. Nieh, and J.S. Stölken, 'Modeling the effect of texture on the deformation mechanisms of nanocrystalline materials at the atomic scale,' *App. Phys. Lett.* 84 (4): 598-600 (2004).

A.M. Hodge and T.G. Nieh, 'Evaluating Abrasive Wear of Amorphous Alloys using Nanoscratch Technique,' *Intermetallics* (2004).

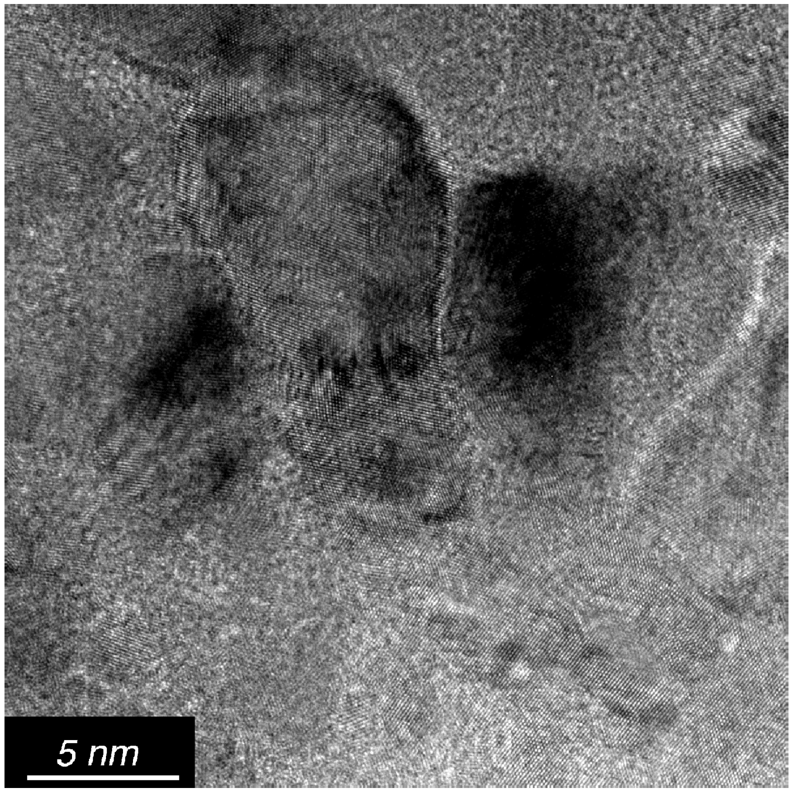

Figure 1 Transmission electron micrographs of electrodeposited nanocrystalline nickel, showing nanoscale grains and the majority of grain boundaries are high-angle.

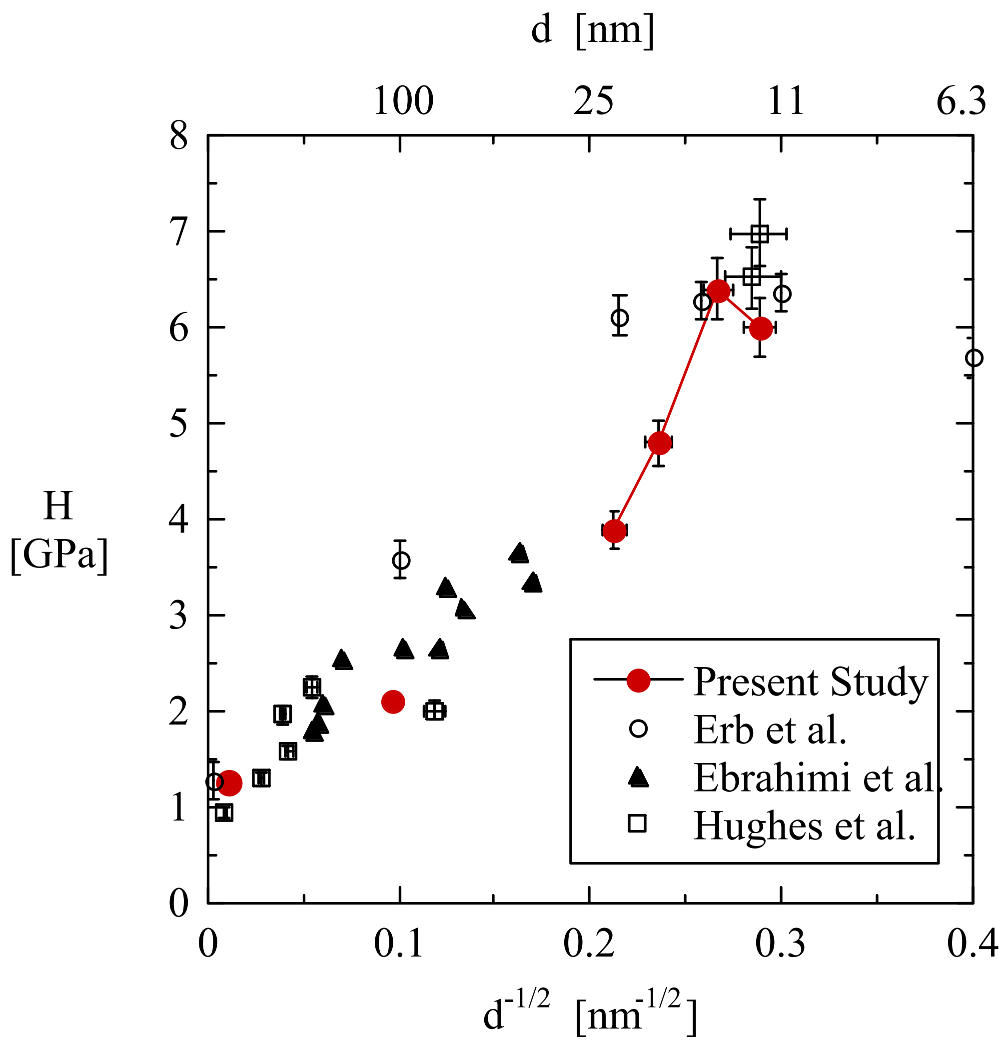

Figure 2: Hall-Petch plot of hardness against the inverse square-root of grain size. The present results are compared with literature, who used electrodeposition to produce nickel specimens.

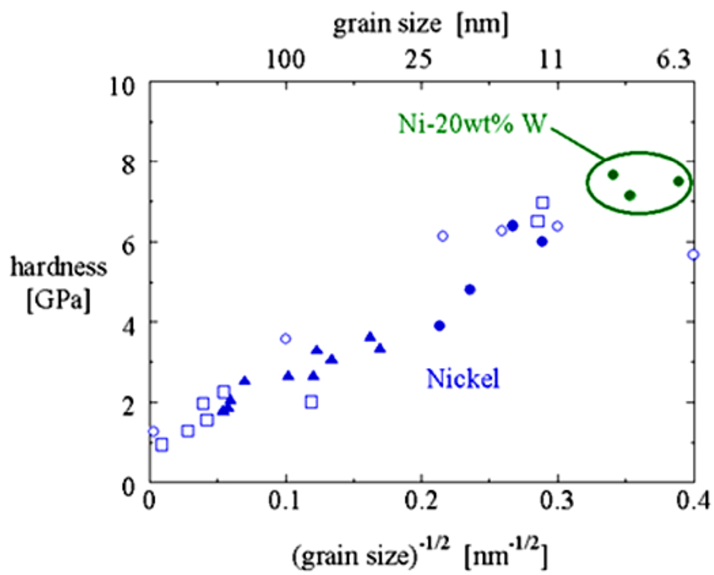

Figure 3. Hall-Petch plot showing the measured hardness of the Ni-W foils as a function of the inverse square-root of grain size. For comparison purposes, data for electrodeposited nickel from literature are also shown.

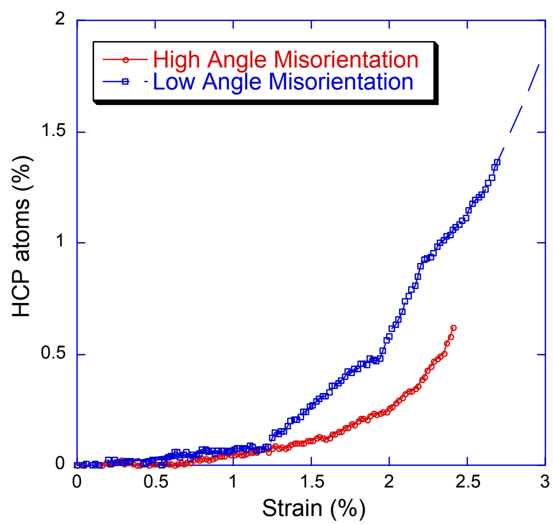

Figure 4: Number of HCP atoms as a function of strain for low angle boundaries (full line) and high angle boundaries (dashed line).

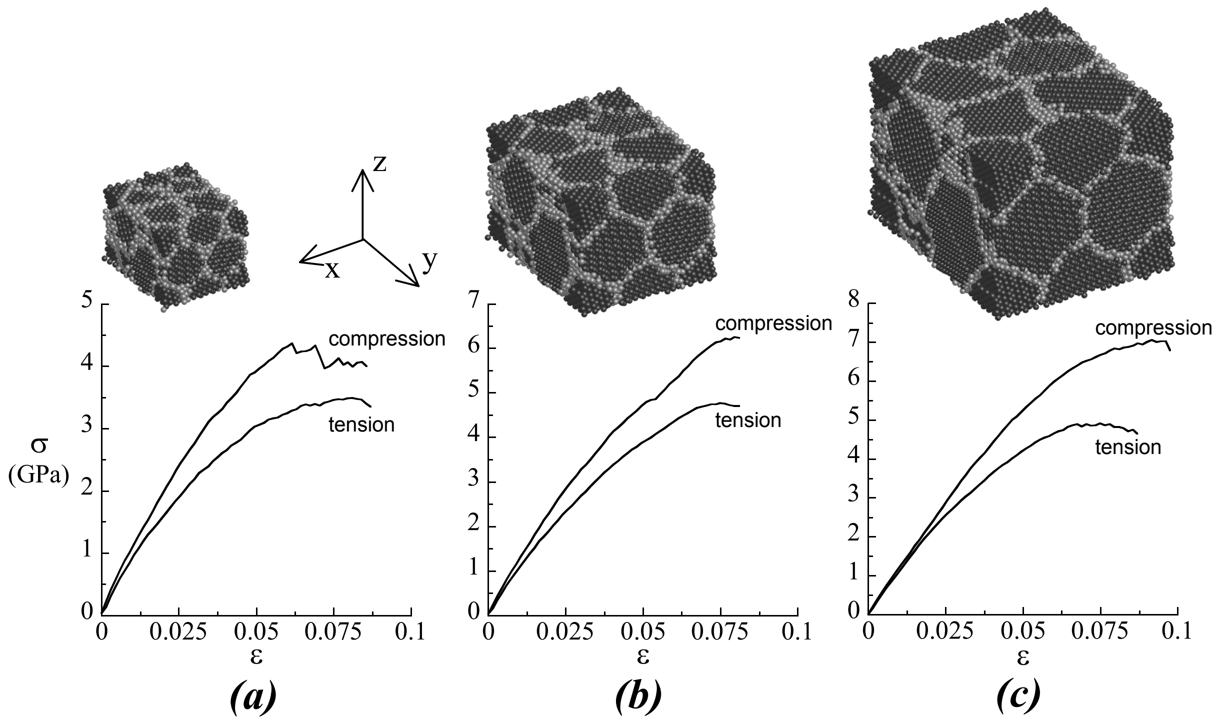

Figure 5: Uniaxial stress-strain (σ–ε) curves of (a) 2 nm, (b) 3 nm, and (c) 4 nm grain size nickel specimens in both tension and compression; views of the structures are also shown, with the grain boundary atoms highlighted for clarity. The curves shown here are for loading along the y-axis.